

Supporting Information

Highly Pt-like activity of Ni-Mo/graphene catalyst for hydrogen evolution from hydrolysis of ammonia borane

Qilu Yao,[#] Zhang-Hui Lu,^{#*} Wei Huang, Xiangshu Chen* and Jia Zhu

Jiangxi Inorganic Membrane Materials Engineering Research Centre, College of Chemistry and Chemical Engineering, Jiangxi Normal University, Nanchang 330022 (P. R. China)

#These authors contributed equally to this work.

**Corresponding author. Email: luzh@jxnu.edu.cn; cxs66cn@jxnu.edu.cn*

1. Experimental

1.1 Chemicals

Ammonia borane (NH_3BH_3 , AB, Aldrich, 90%), Nickel chloride hexahydrate ($\text{NiCl}_2 \cdot 6\text{H}_2\text{O}$, Sinopharm Chemical Reagent Co. Ltd., >98%), sodium molybdate dihydrate ($\text{Na}_2\text{MoO}_4 \cdot 2\text{H}_2\text{O}$, J&K Scientific Ltd., 99.5%), chromic nitrate nonahydrate ($\text{Cr}(\text{NO}_3)_3 \cdot 9\text{H}_2\text{O}$, Aladdin Industrial Inc., 99%), sodium tungstate dihydrate ($\text{Na}_2\text{WO}_4 \cdot 2\text{H}_2\text{O}$, Aladdin Industrial Inc., 99%), graphene (Shanxi Coal Chemical Research Institute of the Chinese Academy of Sciences, $\geq 99.4\%$), and sodium borohydride (NaBH_4 , Aldrich, 99%) were used without further purification. Ultrapure water with the specific resistance of $18.3 \text{ M}\Omega \cdot \text{cm}$ was obtained by reversed osmosis followed by ion exchange and filtration.

1.2 Synthesis of catalysts

The $\text{Ni}_{0.9}\text{Mo}_{0.1}$ /graphene NCs were prepared through a facile chemical reduction method at room temperature. In typical experimental, graphene (6 mg) was firstly dispersed in water (4 mL) with sonication for 30 min to get the well dispersed graphene suspension. And then $\text{NiCl}_2 \cdot 6\text{H}_2\text{O}$ (10.7 mg) and $\text{Na}_2\text{MoO}_4 \cdot 2\text{H}_2\text{O}$ (1.21 mg) were added into the solution, and the mixture was kept stirring for 30 min. The total molar contents of Ni and Mo were kept to be 0.05 mmol. Afterward, 1 mL of fresh aqueous NaBH_4 solution (0.52 M) was added to the above mixture solution with vigorous stirring until the bubble generation ceased. Finally, the black product of $\text{Ni}_{0.9}\text{Mo}_{0.1}$ /graphene could be obtained and used as catalyst for hydrogen generation from the hydrolysis of AB.

The $\text{Ni}_{0.9}\text{Mo}_{0.1}$, Ni/graphene NCs, Ni NPs, $\text{Ni}_{0.9}\text{Cr}_{0.1}$ /graphene, $\text{Ni}_{0.9}\text{Cr}_{0.1}$, $\text{Ni}_{0.8}\text{W}_{0.2}$ /graphene, and $\text{Ni}_{0.8}\text{W}_{0.2}$ samples were also synthesized by the same method.

1.3 Catalyst characterization

Powder X-ray diffraction (XRD) measurements were collected on a Rigaku RINT-2000 X-ray diffractometer using Cu K α radiation source (40 kV, 40 mA) with a scanning angle (2θ) of 10 $^\circ$ -80 $^\circ$. Scanning electron microscope (SEM, Hitachi SU8020), transmission electron microscope (TEM, JEM-2010) and scanning transmission electron microscope (STEM, Titan G2 60-300) equipped with energy dispersive X-ray (EDX) mapping were used for the detailed microstructure of the synthesized samples. The TEM samples were dispersed in ethanol with sonication for 20 min to get the well-dispersed, and few droplets of the nanoparticles suspension were dropped onto the amorphous carbon-coated copper grids. The atomic ratio of Ni : Mo for the Ni-Mo/graphene NCs is measured by inductively coupled plasma-atomic emission spectroscopy (ICP-AES). X-ray photoelectron spectroscopy (XPS) was obtained ESCALABMKLL spectroscope using monochromatized Al K α X-rays as the excitation source. The Ar sputtering experiments were performed under the conditions of background vacuum 3.2×10^{-6} Pa and sputtering acceleration voltage 1 kV. The viscosities of AB with different concentrations were measured with a cone-plate viscometer (Brookfield DV II+ Pro) at 298 K.

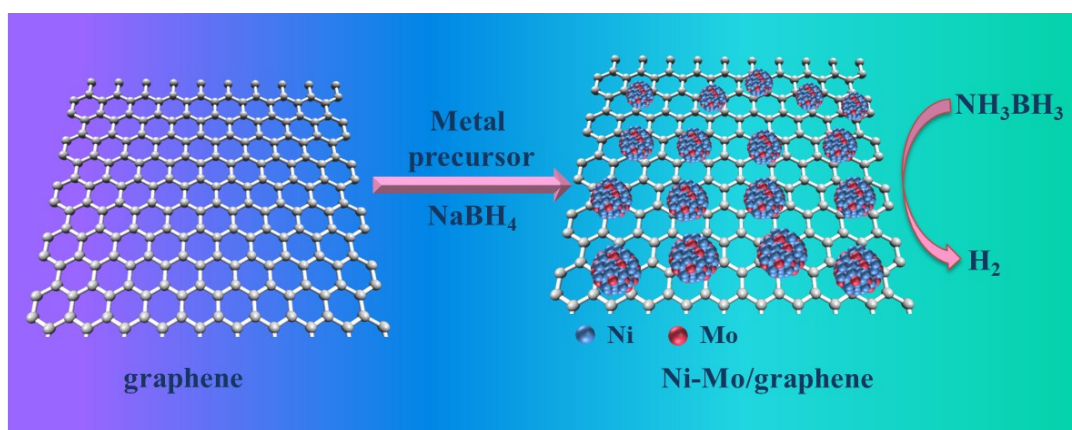
1.4 Catalytic activities of investigations

Reaction apparatus for hydrogen generation from the hydrolysis of AB is the same as previously reported.^{6a} Typically, the as-prepared catalysts were kept in a two-necked round-bottom flask. One neck of the flask was connected to a gas burette to measure the released gas. The catalytic reaction was begun once the 34.3 mg of AB was added into the flask with vigorous magnetic stirring. The evolution of gas was

monitored by recording the displacement of water in the gas burette. The reaction was completed when there was no more gas evolved. In addition, the molar ratios of metal/AB were theoretically kept at 0.05 for all the catalytic reactions, and the reactions were carried out at 298 K under ambient atmosphere.

1.5 Durability test

For the durability test, after the catalytic hydrolytic dehydrogenation of AB was completed, the catalyst was kept in the reaction flask, and a further aliquot of AB (34.3 mg) was subsequently added into flask with vigorous stirring. Such recycle tests of the catalyst for the hydrolysis of AB were carried out for 10 runs at 298 K.



Scheme S1 Schematic illustration for the preparation and application of Ni-Mo/graphene NCs for hydrogen generation from the hydrolysis of AB.

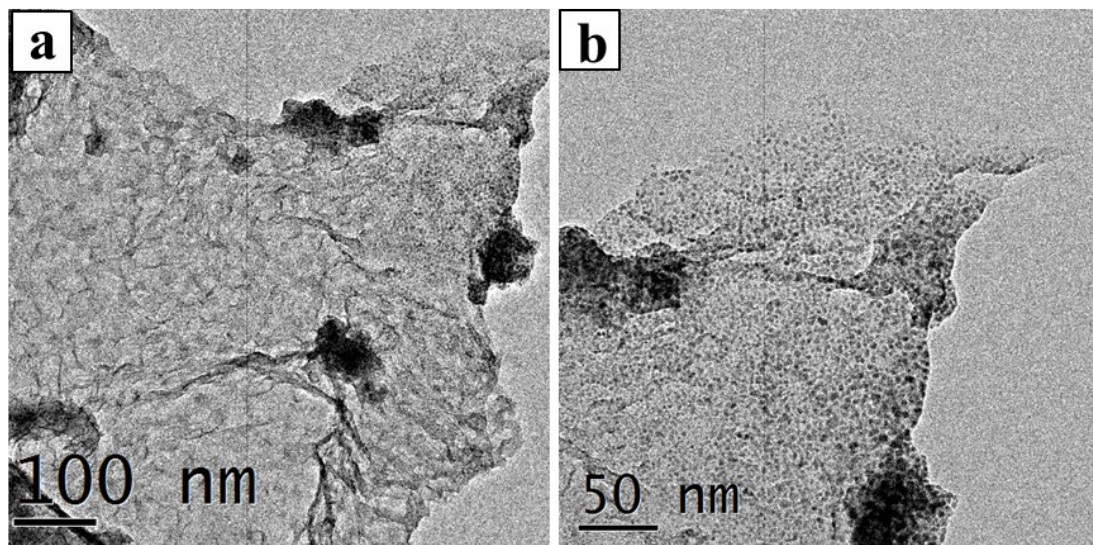


Fig. S1 TEM images for Ni_{0.9}Mo_{0.1}/graphene NCs.

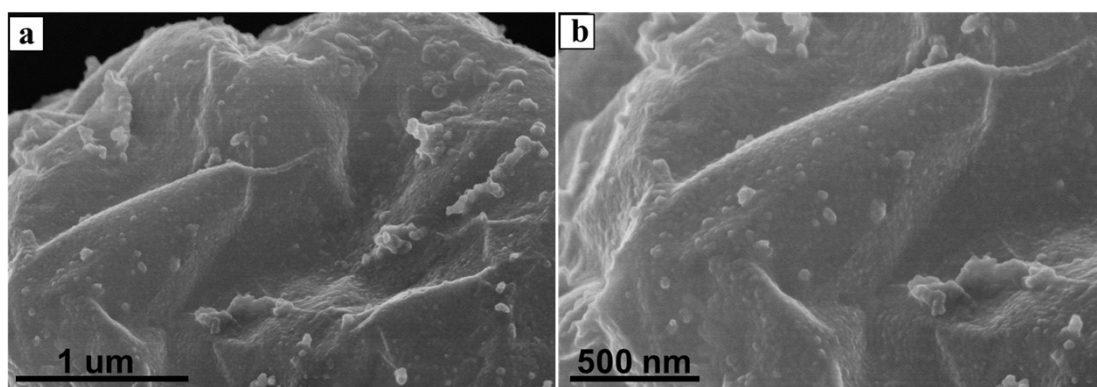


Fig. S2 SEM images for Ni_{0.9}Mo_{0.1}/graphene NCs.

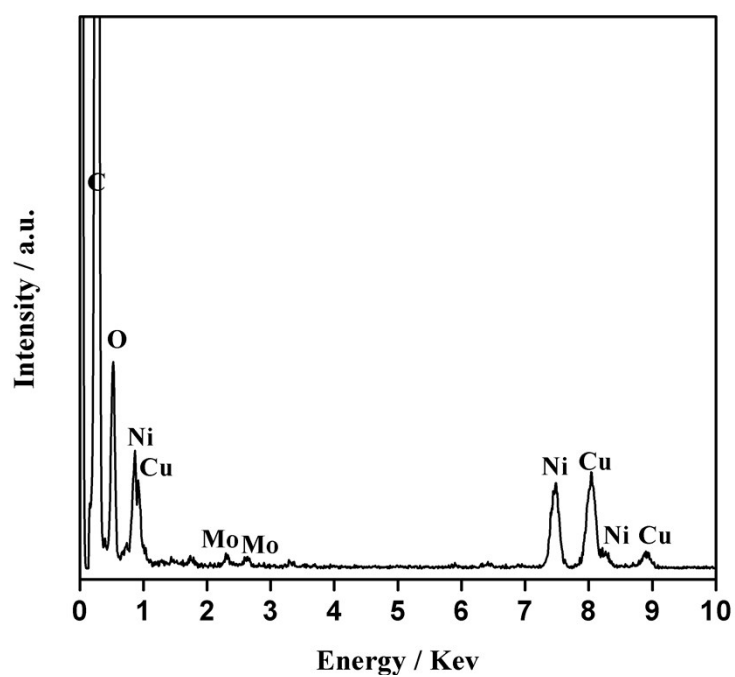


Fig. S3 The corresponding EDX spectrum of the $\text{Ni}_{0.9}\text{Mo}_{0.1}$ /graphene NCs. The Cu signal originates from Cu grid.

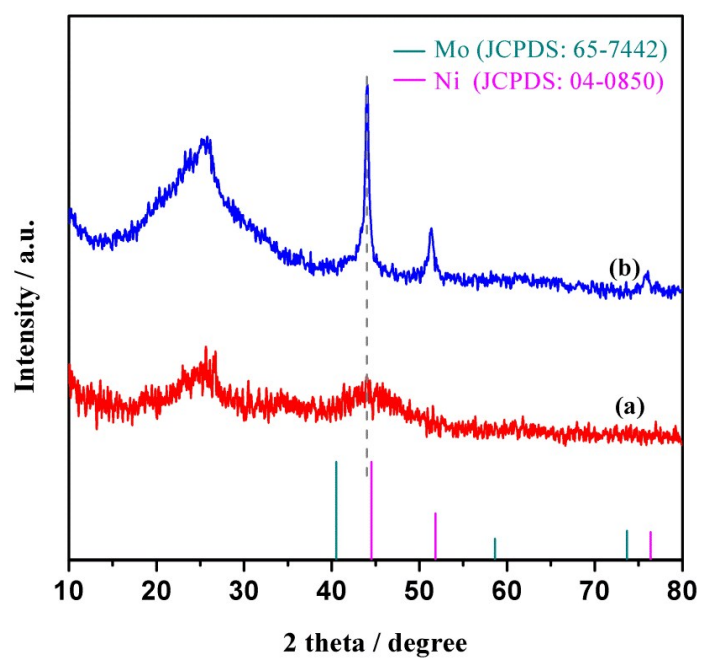


Fig. S4 XRD patterns for the $\text{Ni}_{0.9}\text{Mo}_{0.1}/\text{graphene}$ (a) before and (b) after heat treatment at 823 K for 3 h in Ar atmosphere.

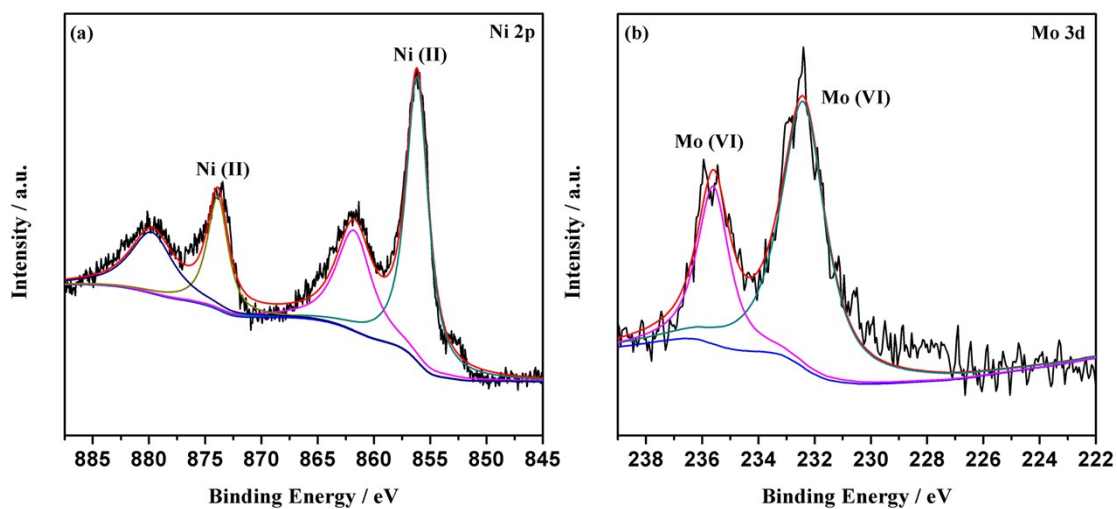


Fig. S5 XPS spectra of (a) Ni 2p and (b) Mo 3d for the $\text{Ni}_{0.9}\text{Mo}_{0.1}/\text{graphene}$ before Ar sputtering.

As shown in Fig. S5, the Ni 2p XPS spectra with the binding energies at 856.16 eV and 873.89 eV can be assigned to oxidized Ni. However, the thin oxidized Ni layer can be readily removed after Ar sputtering for 5 min (Fig. 3). The formation of the oxidized Ni most likely occurs during the sample preparation process for XPS measurements.

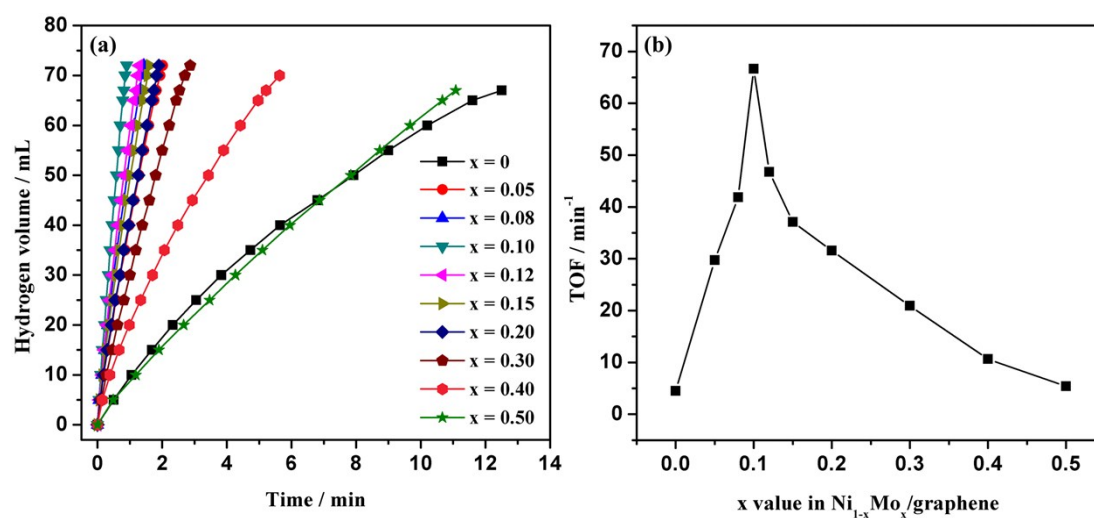


Fig. S6 (a) Plots of time versus volume of hydrogen generated from AB aqueous solution (5 mL, 0.2 M) catalyzed by $\text{Ni}_{1-x}\text{Mo}_x/\text{graphene}$ NCs with different x value and (b) the according TOF values for the hydrolysis of AB at 298 K (metal/AB = 0.05).

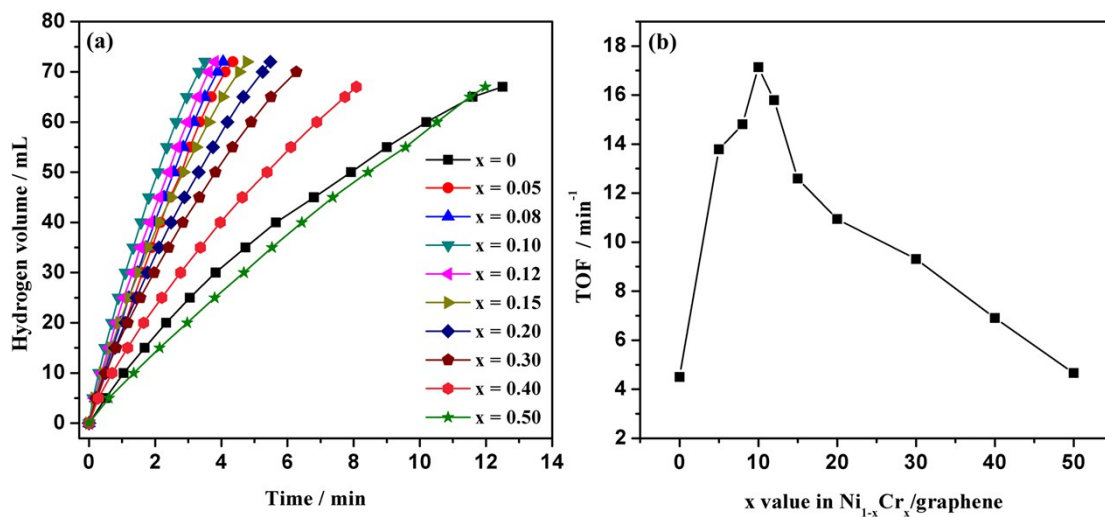


Fig. S7 (a) Plots of time versus volume of hydrogen generated from AB aqueous solution (5 mL, 0.2 M) catalyzed by $\text{Ni}_{1-x}\text{Cr}_x/\text{graphene}$ NCs with different x value and (b) the according TOF values for the hydrolysis of AB at 298 K (metal/AB = 0.05).

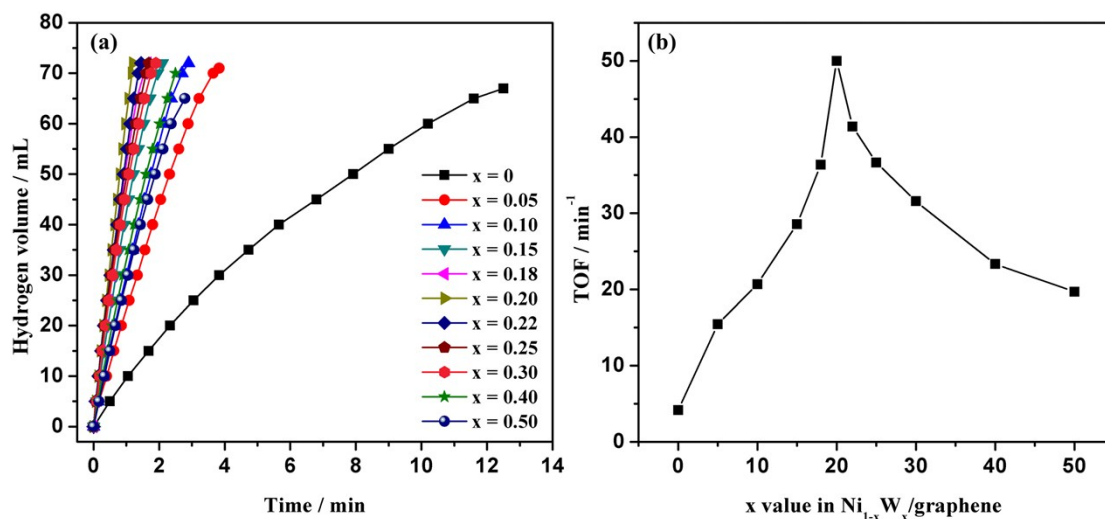


Fig. S8 (a) Plots of time versus volume of hydrogen generated from AB aqueous solution (5 mL, 0.2 M) catalyzed by Ni_{1-x}W_x/graphene NCs with different x value and (b) the according TOF values for the hydrolysis of AB at 298 K (metal/AB = 0.05).

The effect of M (M = Mo, Cr, and W) content on the catalytic activity of Ni_{1-x}M_x/graphene (M = Mo, Cr, and W) NCs was studied by using the catalysts with different molar ratio of Mo (Fig. S6), Cr (Fig. S7), and W (Fig. S8). As shown in Figs. S6-S8, the hydrogen generation rate increased with the increase of Mo, Cr, and W content (x value) of Ni_{1-x}M_x/graphene NCs and the TOF value reaches the maximum with Mo, Cr, and W molar ratio of 0.1, 0.1, and 0.2, respectively, and then further increase the content of M (M = Mo, Cr, and W) lead to the decrease in the hydrogen generation rate. Thus, the catalyst of Ni_{0.9}Mo_{0.1}/graphene, Ni_{0.9}Cr_{0.1}/graphene, and Ni_{0.8}W_{0.2}/graphene NCs was selected to be used in all of the experiments for the further investigation.

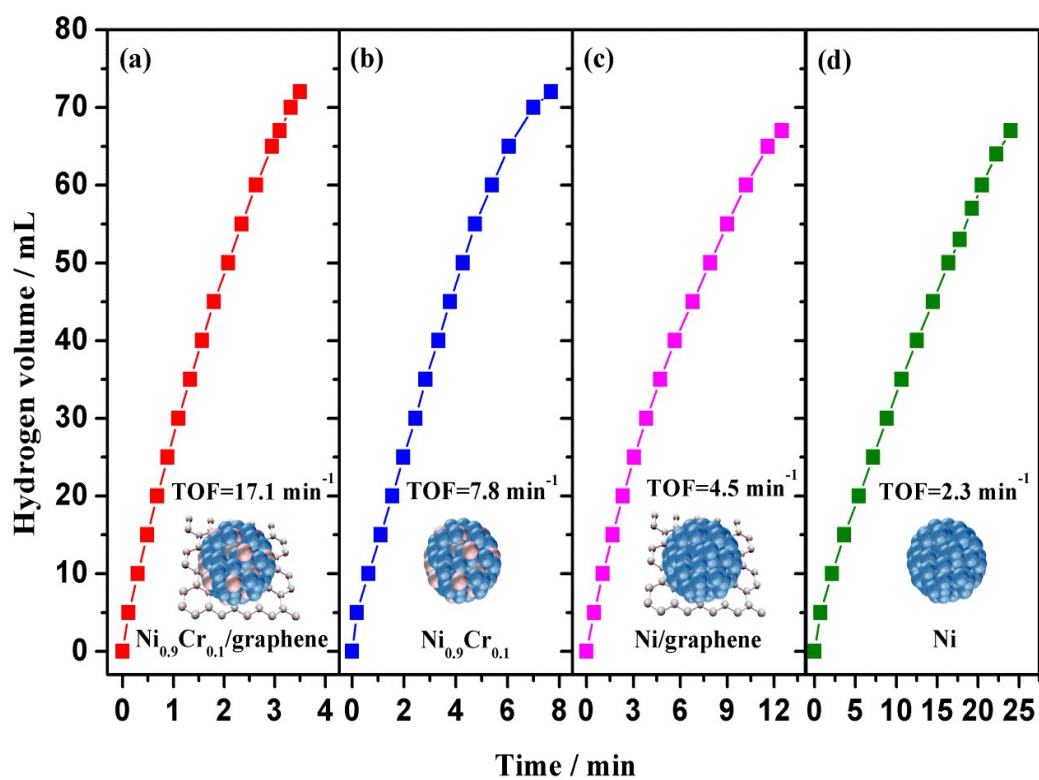


Fig. S9 Plots of time versus volume of hydrogen generated from AB aqueous solution (5 mL, 0.2 M) catalyzed by (a) $\text{Ni}_{0.9}\text{Cr}_{0.1}/\text{graphene}$, (b) $\text{Ni}_{0.9}\text{Cr}_{0.1}$, (c) $\text{Ni}/\text{graphene}$, and (d) Ni at 298 K (metal/AB = 0.05).

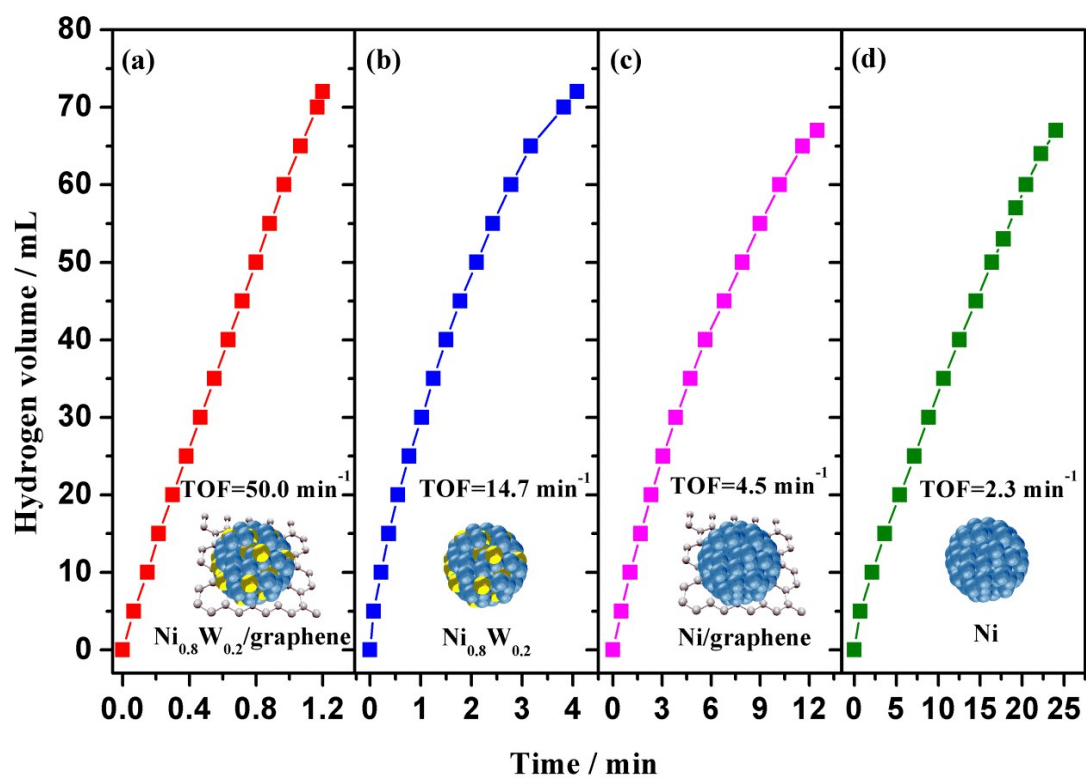


Fig. S10 Plots of time versus volume of hydrogen generated from AB aqueous solution (5 mL, 0.2 M) catalyzed by (a) $\text{Ni}_{0.8}\text{W}_{0.2}/\text{graphene}$, (b) $\text{Ni}_{0.8}\text{W}_{0.2}$, (c) Ni/graphene, and (d) Ni at 298 K (metal/AB = 0.05).

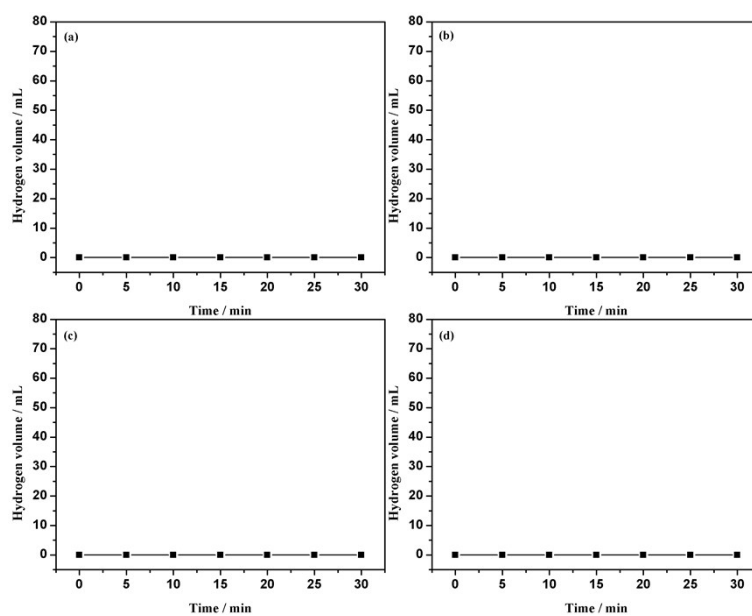


Fig. S11 Plots of time versus volume of hydrogen generated from AB aqueous solution (5 mL, 0.2 M) catalyzed by (a) graphene, (b) Mo/graphene, (c) Cr/graphene, and W/graphene NCs at 298 K (metal/AB = 0.05).

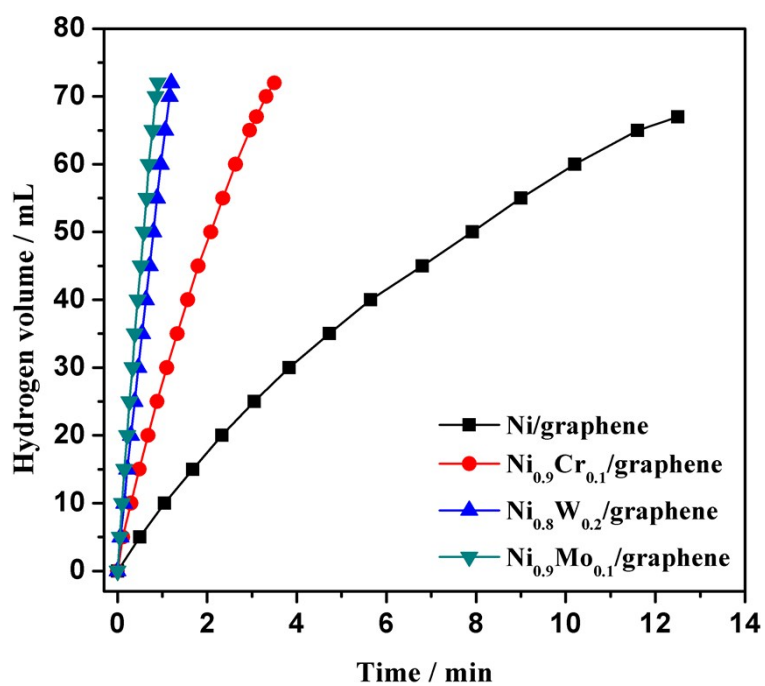


Fig. S12 Plots of time versus volume of hydrogen generated from AB aqueous solution (5 mL, 0.2 M) catalyzed by Ni/graphene, Ni_{0.9}Cr_{0.1}/graphene, Ni_{0.8}W_{0.2}/graphene, and Ni_{0.9}Mo_{0.1}/graphene at 298 K (metal/AB = 0.05).

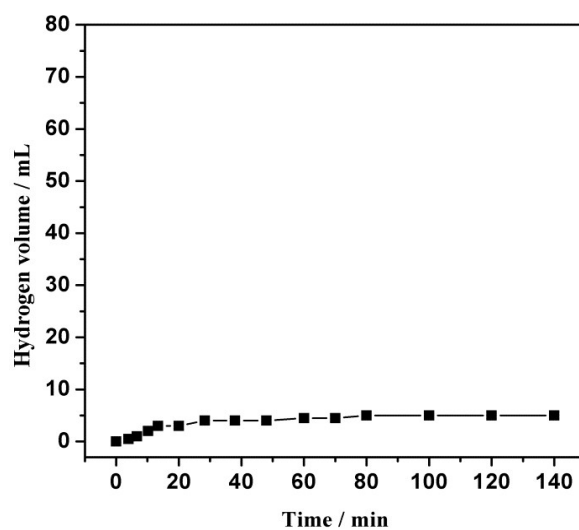


Fig. S13 Plots of time versus volume of hydrogen generated from AB aqueous solution (5 mL, 0.2 M) catalyzed by oxidized Mo (Mo/AB = 0.05).

The oxidized Mo was obtained by thermal decomposition of $(\text{NH}_4)_6\text{Mo}_7\text{O}_{24}\cdot 4\text{H}_2\text{O}$ at 523 K in air for 4 h with the heating rate of $1\text{ }^\circ\text{C min}^{-1}$ (*Advance Materials*, 2015, 27, 4616-4621.). As shown in Fig. S13, the oxidized Mo shows a very low catalytic activity for hydrogen generation from the hydrolysis of AB (only 5 mL of H_2 released within 140 min), suggesting that the oxidized Mo has little effect on the catalytic performance of hydrolysis of AB.

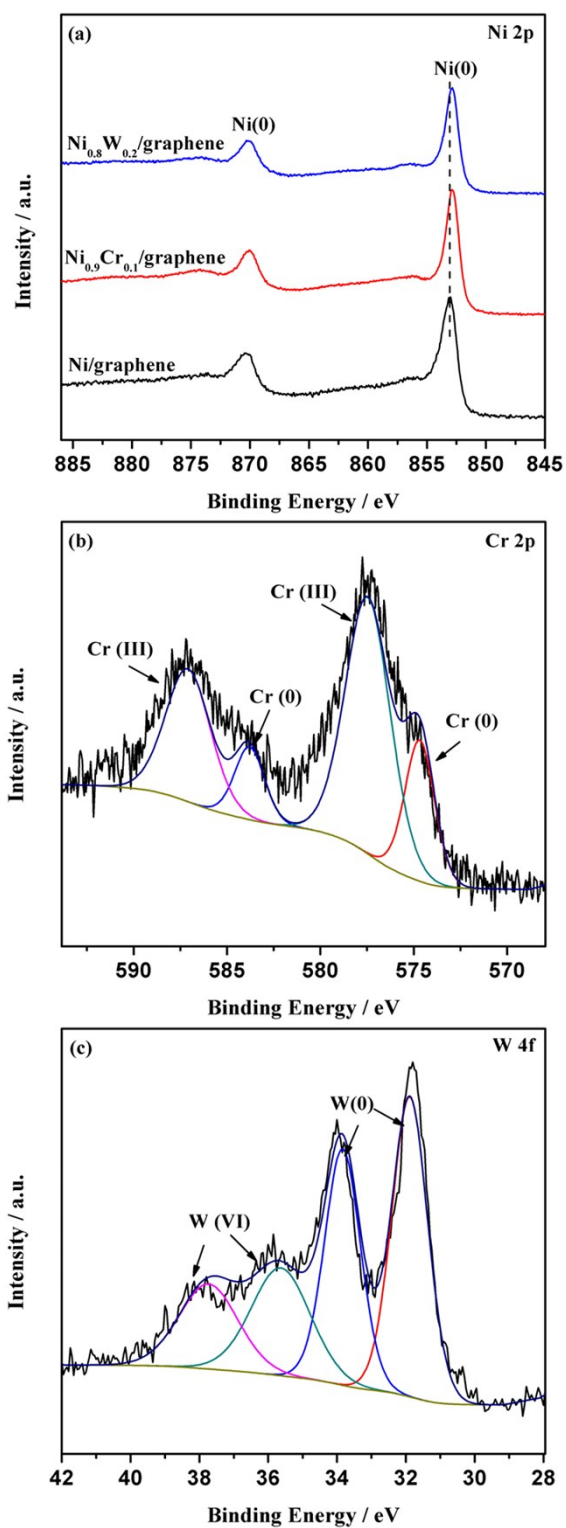


Fig. S14 XPS spectra of (a) Ni 2p for the Ni/graphene, Ni_{0.9}Cr_{0.1}/graphene, and Ni_{0.8}W_{0.2}/graphene, (b) Cr 2p for the Ni_{0.9}Cr_{0.1}/graphene, and (c) W 4f for the Ni_{0.8}W_{0.2}/graphene after Ar sputtering.

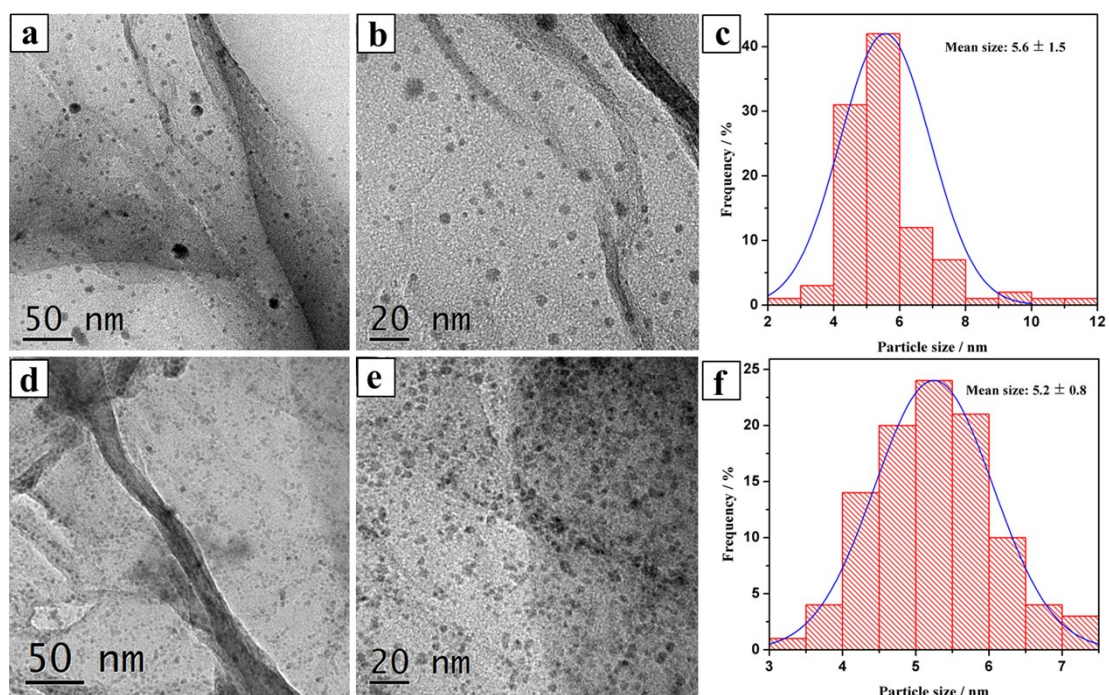


Fig. S15 TEM images for (a,b) Ni_{0.9}Cr_{0.1}/graphene and (d,e) Ni_{0.8}W_{0.2}/graphene NCs; Particle size distributions for the (c) Ni_{0.9}Cr_{0.1}/graphene and (f) Ni_{0.8}W_{0.2}/graphene NCs.

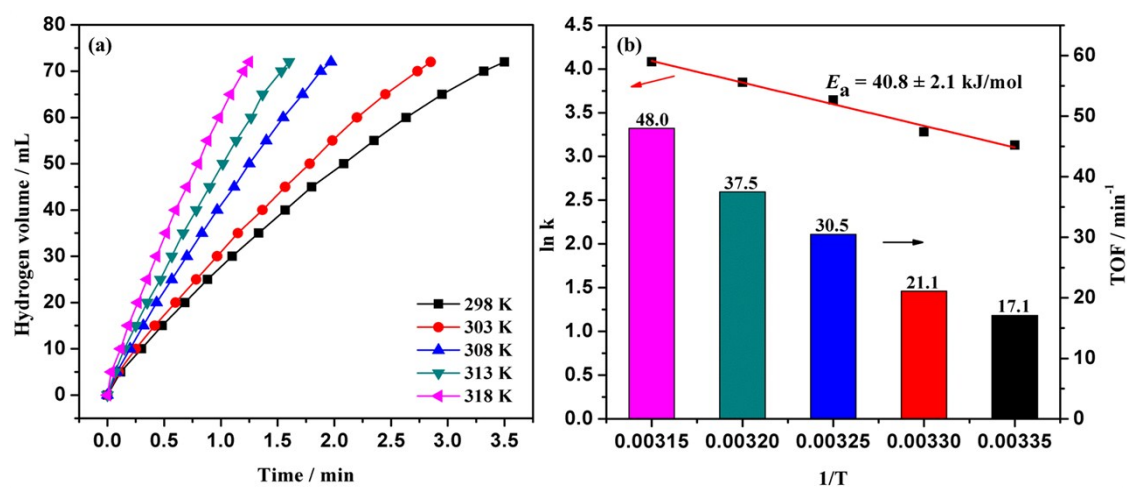


Fig. S16 (a) Plots of time versus volume of hydrogen generated from AB aqueous solution (5 mL, 0.2 M) and (b) Arrhenius plots and TOF values of AB hydrolytic dehydrogenation catalyzed by Ni_{0.9}Cr_{0.1}/graphene NCs at different temperatures (metal/AB = 0.05).

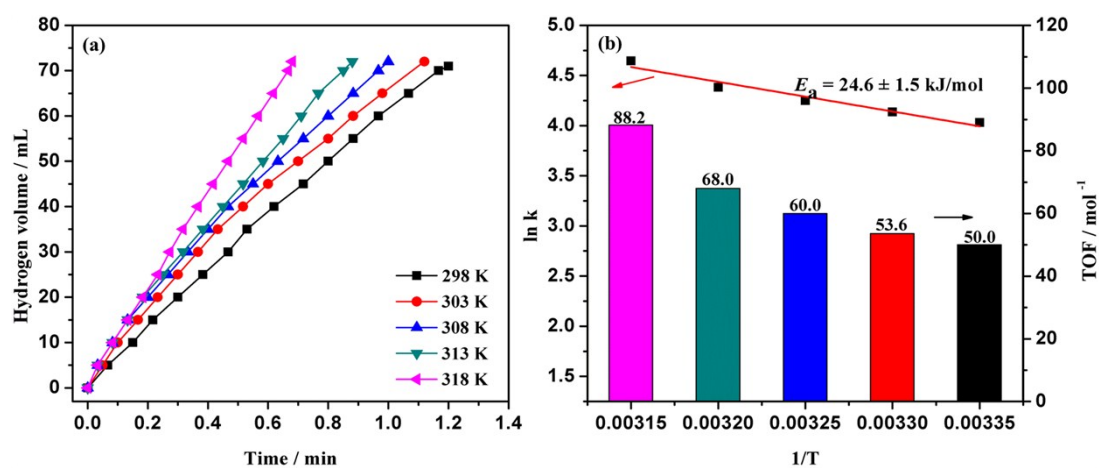


Fig. S17 (a) Plots of time versus volume of hydrogen generated from AB aqueous solution (5 mL, 0.2 M) and (b) Arrhenius plots and TOF values of AB hydrolytic dehydrogenation catalyzed by Ni_{0.8}W_{0.2}/graphene NCs at different temperatures (metal/AB = 0.05).

Table S1 The values of activation energy (E_a) for hydrogen evolution from the hydrolysis of AB catalyzed by different catalysts.

Catalyst	E_a (kJ/mol)	Ref.
NiCo alloy hexagonal plates	49.4	7g
Ni ₃₀ Pd ₇₀ /rGO	45	S1
Ni ₂ P	44.6	8c
Cu _{0.5} Ni _{0.5} /CMK-1	43	7d
Ni_{0.9}Cr_{0.1}/graphene	40.8	This work
Cu/RGO	38.2	S2
CuNi/MCM-41	38	S3
Ni _{0.74} Ru _{0.26} alloy	37.18	S4
Ni/SiO ₂	34	7e
Ni@meso-SiO ₂ spheres	29	S5
3.2 nm Ni/C	28	8d
Nanoporous Ni spheres	27	8e
Ni_{0.8}W_{0.2}/graphene	24.6	This work
Ru/ γ -Al ₂ O ₃	23	5a
Ni_{0.9}Mo_{0.1}/graphene	21.8	This work
Rh/ γ -Al ₂ O ₃	21	5a
Pt/ γ -Al ₂ O ₃	21	5a

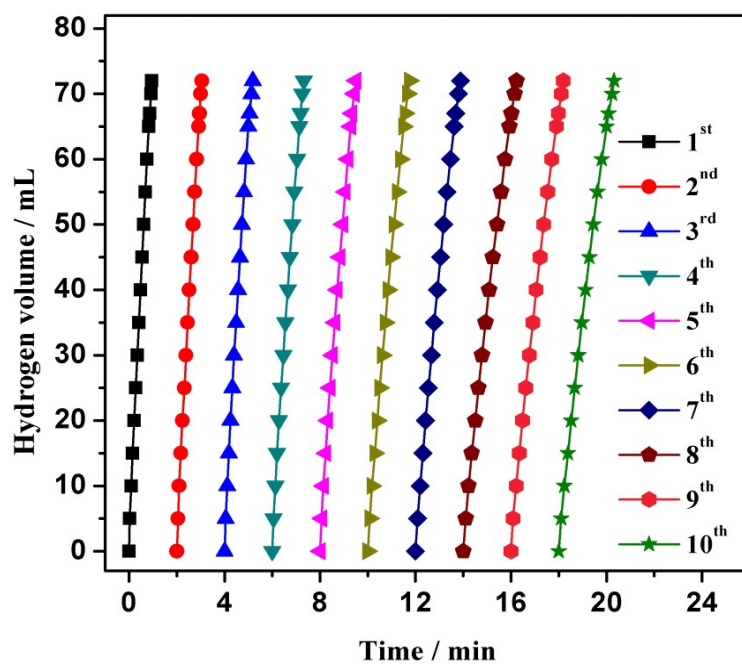


Fig. S18 Durability test for hydrogen generation from AB aqueous solution (5 mL, 0.2 M) catalyzed by Ni_{0.9}Mo_{0.1}/graphene NCs at 298 K (metal/AB = 0.05).

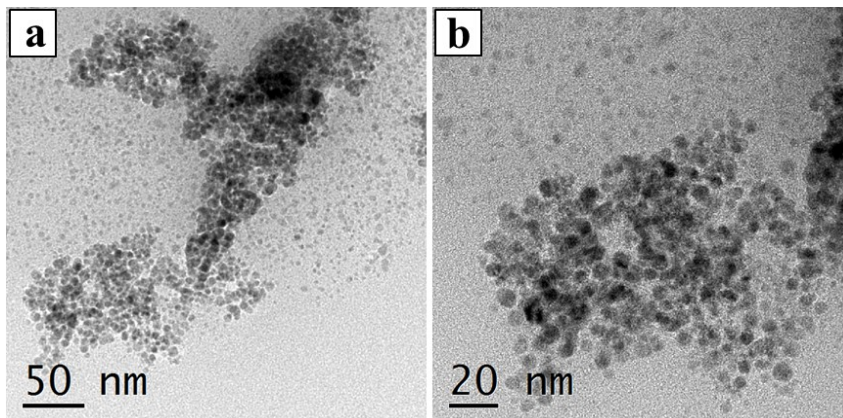


Fig. S19 TEM images for Ni_{0.9}Mo_{0.1}/graphene NCs after the durability test for hydrogen generation from AB aqueous solution.

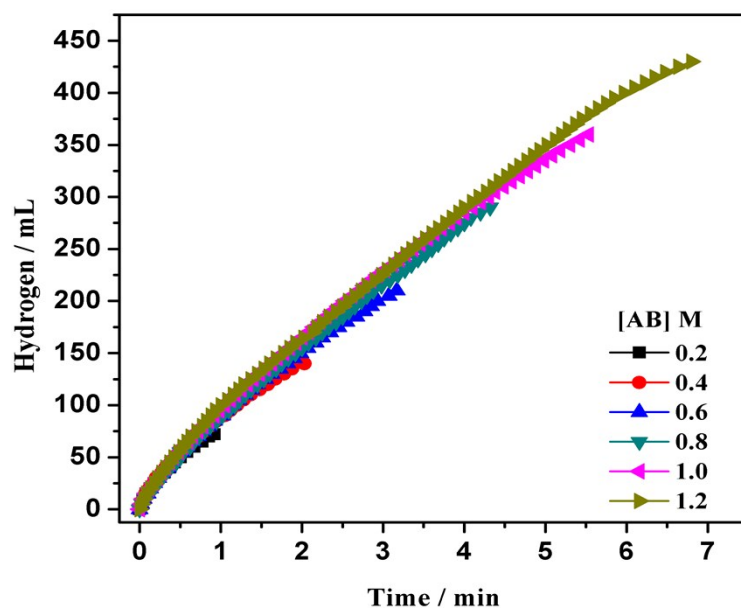


Fig. S20 Plots of time versus volume of hydrogen generated from the hydrolysis of AB starting with different initial concentrations of AB (5 mL, x M) while keeping the concentration of Ni_{0.9}Mo_{0.1}/graphene (0.01 M) at constant under 298 K.

As shown in Fig. S20, it is found that by increasing the AB concentration from 0.2 to 1.2 M (the corresponding viscosity is in the range from 6.9 to 11.2 mPa·s, see Table S2), the hydrogen generation rates do not change significantly, but the total turnover frequency (TOF) of reactions show a slightly decreases (Table S2), which can be ascribed to the increase in viscosity of reaction solution.

Table S2. The viscosity values (η) and catalytic activities for aqueous solution of AB with different concentrations at 298 K.

AB/[M]	η /mPa·s	H ₂ /mmol	t/min	TOF/min ⁻¹
0.2	6.9	3	0.9	66.7
0.4	7.5	6	2.0	60.0
0.6	8.6	9	3.2	56.2
0.8	9.5	12	4.3	55.8
1.0	10.3	15	5.5	54.5
1.2	11.2	18	6.8	52.9

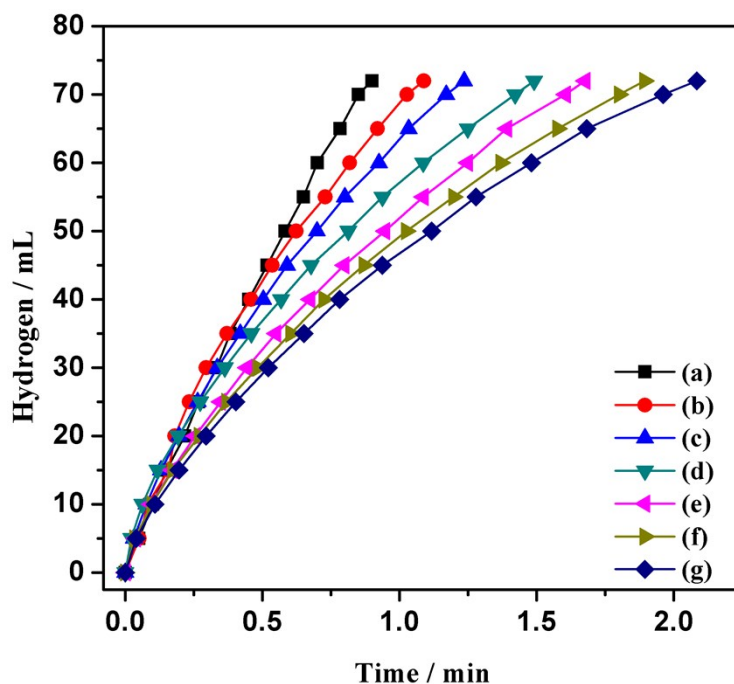


Fig. S21 Plots of time versus volume of hydrogen generated from AB (1 mmol) aqueous solution catalyzed by $\text{Ni}_{0.9}\text{Mo}_{0.1}$ /graphene NCs without added generated products (a) and with added 5 mL of generated products from the hydrolysis of different AB concentrations (b) 0.2 M, (c) 0.4 M, (d) 0.6 M, (e) 0.8 M, (f) 1.0 M, and (g) 1.2 M at 298 K (metal/AB = 0.05).

After catalytic reaction, the generated products of the reactions were collected by centrifugation. The effect of the generated products on the catalytic performance of $\text{Ni}_{0.9}\text{Mo}_{0.1}$ /graphene NCs was also studied by performing a series of experiments with varying the above generated products from the hydrolysis of different AB concentrations (0.2-1.2 M) while keeping the AB (1 mmol) and $\text{Ni}_{0.9}\text{Mo}_{0.1}$ /graphene NCs content (metal/AB = 0.05) unchanged. As shown in Fig. S21, the hydrogen generation rates are slightly decreased with the increased concentration of the generated products from AB, probably due to the increased viscosity of the reaction solution or the increasing metaborate concentration of the generated products.

Calculation method for *TOF*:

The total turnover frequency (*TOF*) reported in this work is an apparent *TOF* value based on the number of metal atoms in catalyst, which is calculated from the equation as follow:

$$TOF = \frac{nH_2}{n_{metal} \times t} \quad (S1)$$

Where nH_2 is the mole number of generated H_2 , n_{metal} is the mole number of metal (Ni and Mo) in catalyst and t is the completed reaction time in minute.

References

- (S1) Çiftci, N. S.; Metin, Ö. *Int. J. Hydrogen Energy* **2014**, *39*, 18863–18870.
- (S2) Yang, Y.; Lu, Z. H.; Hu, Y.; Zhang, Z.; Shi, W.; Chen, X.; Wang, T. *RSC Adv.* **2014**, *4*, 13749–13752.
- (S3) Lu, Z. H.; Li, J.; Feng, G.; Yao, Q.; Zhang, F.; Zhou, R.; Tao, D.; Chen, X.; Yu, Z. Q. *Int. J. Hydrogen Energy* **2014**, *39*, 13389–13395.
- (S4) Chen, G.; Desinan, S.; Rosei, R.; Rosei, F.; Ma, D. *Chem. Eur. J.* **2012**, *3*, 7925–7930.
- (S5) Liu, H.; Cao, C.; Li, P.; Yu, Y.; Song, W. *J. Energy Chem.* **2014**, *23*, 50–56.